Journal of the Meteorological Society of Japan,Vol. 77, No. 1B, pp. 217–234, 1999

Simulations of Soil Moisture and Surface Water Balance Using the Simple Biosphere Model 2

By Changan Zhang, Donald A. Dazlich and David. A. Randall

Department of Atmospheric Science, Colorado State University, Fort Collins, CO 80523, U.S.A.

(Manuscript received 24 February 1998, in revised form 4 February 1999)

Abstract

Soil moisture and water balance for global and regional scales have been calculated using a land-surface process model (SiB2) forced by observed and model assimilated data. The simulated runoff for each grid cell has been provided as input to a global river routing model, in order to simulate river discharge rates. The simulated soil moisture and water balance have been compared with available observations for their annual mean and seasonal cycles and for global, basin and grid point scales. The global distributions of the annual-mean soil moisture and wetness have been reasonably simulated. There were large inter-annual variations of soil moisture in both the simulations and observations at local stations. The simulated annual discharges for major river basins agree reasonably well with observations, but with some underestimates for large discharges and some overestimates for small discharges. The seasonal cycle of river discharges has been well simulated for specific basins in the tropics, midlatitudes, and high latitudes, although for some basins the annual mean is underestimated. In the tropics, the seasonal cycles of soil moisture and the surface water balance are dominated by the precipitation cycle. In mid- and high latitudes, soil moisture and the water balance are affected by both the temperature and precipitation cycles, and by the snow accumulation/melting cycle. The range of seasonal soil moisture variations becomes smaller with increasing latitude. The seasonal cycles of soil moisture for selected grid points have been compared with selected station observations. Even though there are differences in forcing and in some specific surface boundary parameters at the stations, the simulated soil moisture agrees well with multiyear observations at a majority of the stations. However, for almost all the selected grid cells, the seasonal variations are smaller, the snow melt and soil drying processes are late by about one month, and the soil is relatively wet in summer, compared with observations. These errors can be partly attributed to the unrealistically cool temperatures provided to the model as forcing data, favoring less surface evaporation and a later seasonal cycle, especially for mid- and high latitudes.

1. Introduction

Soil wetness helps determine the partitioning of surface available energy between the sensible and latent heat fluxes. This partitioning affects boundary layer turbulence, cloudiness, and precipitation. Numerical simulations have demonstrated that the climate is sensitive to soil moisture anomalies (Betts *et al.*, 1994; Kunkel *et al.*, 1994; Dirmeyer, 1994; Fennessy *et al.*, 1994; Delworth and Manabe, 1988 and 1989; Rowntree and Bolton, 1983; Rind, 1982; Shukla and Mintz, 1982). Soil moisture is also important for hydrometeorological and ecological processes (Denning *et al.*, 1996).

Soil moisture affects the atmosphere on a variety of time scales. Using the weather forecasting model of the European Centre for Medium Range Weather Forecasts (ECMWF), Betts *et al.* (1994) found that, with a higher initial soil moisture content, more realistic precipitation and surface temperature patterns were produced for the 1993 summer floods in central North America. Soil moisture can affect seasonal surface water balance as well. The above-normal soil wetness in spring 1993 may have contributed to the 1993 summer flood, according to the analysis of Kunkel *et al.* (1994). On the other hand, lower initial spring soil wetness may lead to less surface evaporation and thus to a summer drought situation as simulated by Oglesby (1991), Dirmeyer (1994) and Fennessy *et al.* (1994).

Corresponding author: Donald Dazlich, Colorado State University, Department of Atmospheric Science, Fort Collins, CO 80523-1371, U.S.A. E-mail: dazlich@atmos.colostate.edu

Until recently, bucket models were widely used to parameterize the surface energy and soil water balances in offline calculations (Budyko, 1956; Mintz and Serafini, 1981 and 1992) and in general circulation models (GCMs; Manabe, 1969; Arakawa, 1972; Washington and Meehl, 1984). A bucket model is an idealized soil water balance model in which the available soil moisture, with a fixed field capacity (typically 150 mm), is determined by a balance between precipitation into the bucket and water losses through surface evapotranspiration and runoff. In a study of the land-surface water balance, Mintz and Serafini (1981 and 1992) simplified their bucket model by neglecting the snow-melt term. This simplifying assumption can distort the soil water balance in mid- and higher latitude regions.

In a bucket model, the simulated soil moisture is affected by the field capacity, because evaporation and runoff are assumed to depend on the amount of moisture in the bucket. The subgrid distribution of precipitation must also be considered, because interception loss, infiltration, and runoff differ between large-scale stratiform precipitation and localized convective precipitation. Wood *et al.* (1992) tested a improved bucket model with variable subgrid infiltration, and found that the simulated surface hydrology was more realistic, particularly in terms of reduced short-term soil moisture fluctuations, relative to the original bucket model.

More comprehensive land surface process models have been developed during the past ten years, including the Biosphere-Atmosphere Transfer Scheme (BATS; Dickinson, 1984) and the Simple Biosphere model (SiB; Sellers *et al.*, 1986; Sellers *et al.*, 1996a). In these models, the control of transpiration by vegetation is modeled explicitly. Water movement between soil layers is better represented, as shown by Abramopoulos *et al.* (1988). Sato *et al.* (1989) published results from simulations using the first version of SiB (SiB1), as incorporated into the Center for Ocean-Land- and Atmosphere version of the U.S. National Meteorological Center's GCM. They showed that the surface fluxes of energy, momentum, heat and moisture were in reasonable agreement with the available field observations. Randall *et al.* (1996) reported the results of simulations using a new version of SiB (SiB2) coupled to the Colorado State University (CSU) GCM. These simulations were compared with the results of a control simulation which used a bucket model similar to that of Manabe (1969). The two versions of the model used the same surface albedo and roughness length distributions, however. Generally, SiB2 produces a warmer and drier surface and atmospheric boundary layer than the bucket model. Compared with the control run, the coupled system produced less cloud cover over land and increases in the surface absorbed shortwave radiation and longwave cooling, as well as less continental precipitation and stronger spatial variations in soil wetness.

Using an offline version of SiB2, called "SiBDRV," which is driven by data obtained from ECMWF's analysis-forecast system and observed precipitation, Zhang *et al.* (1996) reported simulations of the surface energy budget including latent heat flux. They compared the SiBDRV results with those obtained using the CSU GCM, coupled with exactly the same version of SiB2, and also with the surface fluxes provided as part of the original ECMWF model output. The comparisons were encouraging and suggested that we may be able to analyze the surface water budget in more detail.

In this paper, we report analyses of the SiBDRV results for the global soil moisture and water balance, as in the study of Zhang *et al.* (1996). We compare the model results with observations based on satellite remote sensing and station data. This investigation is part of an intercomparison of analyses of the global soil moisture, as organized by the ISLSCP (International GEWEX Project Office, 1995). A key objective of the GEWEX study is to develop estimates of the global climatology of soil moisture by driving land-surface models with the observed state of the atmosphere. An important step towards this goal is the estimation of the soil moisture for the years 1987 and 1988.

This study attempts, we are trying to answer the following questions: Can we simulate the global soil moisture and surface water balance using a land surface model forced with "observed" meteorological data and surfaceboundary conditions? On what spatial and temporal scales can soil moisture and land surface water balance be simulated well compared with observations? The spatial scales we examine range from global to catchment scale. The two years of forcing data available limit the temporal scales that can be addressed, and so we focus on seasonal scales.

In Section 2, we briefly describe SiB2 and its surface hydrological submodel, and a river routing model used to analyze river basin water balance. The design of our numerical simulations is discussed in Section 3. Section 4 presents the simulated soil moisture and water balance for global, regional, and local scales. Comparisons of the simulated soil moisture and water balance with observations were made to address the questions. A summary and conclusions are given in Section 5.

2. SiB2 and a river routing model

2.1 SiB2 surface water balance

As discussed by Sellers *et al.* (1996a), SiB2 includes one canopy layer, and three soil layers: a surface soil layer, a root zone, and a deep soil layer. A canopy photosynthesis submodel (Collatz *et al.*, 1990, 1991, and 1992; Sellers *et al.*, 1992) has been

incorporated, with a prognostic stomatal conductance and a diagnostic calculation of the photosynthetic CO_2 flux between the atmosphere and the land-surface. A new patchy snow parameterization has also been included.

SiB2 has ten prognostic variables: the vegetation canopy temperature (T_c), the temperature of the first 2 cm of the soil at the surface (T_g), a deep soil temperature profile distributed in six layers from 2 cm to 6 m soil depth (T_{D1}, T_{D2}, $\cdots$, T_{D6}); the mass of water intercepted on the canopy (S_{cw}) and on the surface soil layer (S_{gw}); the mass of snow intercepted on the canopy (S_{cs}) and on the surface soil layer (S_{gs}); and the surface soil wetness (W_1), root-zone soil wetness (W_2), and deep soil wetness (W_3). Following Sellers *et al.* (1986 and 1996a), the soil water balances in the three soil layers are expressed by

$$\frac{\partial W_1}{\partial t} = \frac{1}{\theta_S D_1}\left[(D_d + D_c) + S_{mlt} - R_o - Q_{1,2} - E_{gs}\right], \quad (1)$$

$$\frac{\partial W_2}{\partial t} = \frac{1}{\theta_S D_2}\left[Q_{1,2} - Q_{2,3} - E_{ct}\right], \quad (2)$$

$$\frac{\partial W_3}{\partial t} = \frac{1}{\theta_S D_3}\left[Q_{2,3} - Q_3\right], \quad (3)$$

where θ_s is the saturation volumetric soil moisture (soil porosity), which depends on soil type, and the $D_i (i = 1, 2, 3)$ the soil depths for the surface soil, root-zone, and deep soil layers. D_d is the canopy throughfall rate of precipitation, and D_c is the canopy drainage rate of the intercepted precipitation. S_{mlt} is the rate of snow melt. $Q_{i,i+1}$, where $i = 1, 2$, represents the rates of exchange water flux between two soil layers. Q_3 is the gravitational drainage rate at the bottom of the deep soil layer. R_o is surface runoff due to excess water infiltration at the surface soil layer. The total runoff is $R = R_o + Q_3$.

The evapotranspiration rate in SiB2 consists of four components that are controlled by distinct biophysical processes: the evaporation rates from canopy and ground interception stores, E_{ci} and E_g, respectively. In Eq. (2) and (3), E_{gs} is evaporation rate from soil surface layer; and E_{ct} is canopy transpiration rate through the stomata.

As described by Sellers *et al.* (1992 and 1996a), canopy photosynthesisis explicitly modeled in SiB2. The canopy carbon assimilation rate is regulated in three ways: rubisco-limitation, light-limitation, and transport-limitation. The plant takes in CO_2 and releases water vapor through its stomata. The stomatal conductance is expressed as a function of the net assimilation rate and the CO_2 concentration at the leaf surface, as discussed by Collatz *et al.* (1991 and 1992) and Sellers *et al.* (1992 and 1996a). Canopy transpiration of water vapor is directly related to canopy carbon assimilation through the canopy conductance. Transpiration in turn may feedback on the canopy conductance by affecting the canopy's environment.

The effects of the subgrid convective precipitation on the surface hydrology are parameterized in SiB2. Convective precipitation tends to produce more canopy throughfall and surface runoff, relative to large-scale or stratiform precipitation (Sato *et al.*, 1989; Sellers *et al.*, 1996a).

Canopy storage capacity is a function of the leaf area index (LAI), and the soil surface storage capacity for interception is assumed to be limited to 0.2 mm for liquid water (S_{gw}) and unlimited for snow accumulation (S_{gs}). The intercepted water and soil moisture are then available to supply the various surface moisture fluxes (E_{ci}, E_{gi}, E_{gs}, and E_{ct}).

When snow falls, it is treated as large-scale precipitation. Snow can accumulate without limit on the ground surface, but canopy snow interception is limited, depending on the LAI. Snow accumulation and melting affect the surface energy balance, surface roughness, and soil moisture balance. In this study, precipitation is assumed to be snow when the temperature in the atmospheric boundary layer is below freezing.

2.2 River routing model

The river routing model used in this study is identical to the model developed by Miller *et al.* (1994). The model considers one surface reservoir, and an effective flow speed of water from one grid point to its downstream neighbor. A single globally uniform flow speed was used based on optimizing the simulated and observed river discharges. In this study, we chose to use 0.5 m s^{-1}, which is the value Miller *et al.* (1994) found minimized the global discharge error for a hydrology model that included groundwater runoff. The river speed used apparently is slower than real river flow because we assume that surface and ground runoff reach river bed at the same speed. The global river speed value was corrected by a local topographic slope. In this study, the maximum and minimum river speed were limited to 5.0 and 0.25 m s^{-1}, respectively.

Inputs to the river routing model are total runoff rate simulated by SiB2 and a global river direction data file called: Total Runoff Integrating Pathways (TRIP), at 1 × 1 degree resolution (Oki and Sud, 1998). TRIP recognizes a total of about 200 rivers distributed over the globe.

3. Computational design

The SiBDRV simulations consist of two parts, covering 1987 and 1988. The first part is a ten-year run forced by the observed six-hourly precipitation, which was the monthly observed precipitation inter-

polated into six-hourly values according to the six-hourly forecasted precipitation from the NCEP (the National Centers for Environmental Prediction) regional forecasting model, and by surface meteorological data produced by the ECMWF analysis-forecast system. The run began with a ten-year simulation, with repeating 1987 conditions. The second part started from the end of 1987, and continued for one year with 1988 conditions. The last two simulated years are analyzed for this study.

Six-hourly ECMWF data were used to specify the atmospheric and radiative forcings. The data started on January 1, 1987, and ended on December 31, 1988. The data were provided at 1 × 1-degree resolution through the ISLSCP Initiative I data sets (Sellers *et al.*, 1996c). Corresponding biophysical and soil parameters, used as boundary conditions by SiB2, were based upon a number of data sets, including satellite data (Sellers *et al.*, 1996b), and were also distributed through the ISLSCP Initiative I data sets.

The initial soil moisture was set to 75 % of soil saturation. After ten years of 1987 forcing, the soil moisture reached a seasonally repeating equilibrium. This equilibrium was established by comparing successive December 31 soil moisture states of the surface and root zones. The criterion for convergence of the spin-up was that the difference between successive December 31 states was less than 5 % or 5 mm, whichever was less stringent, at every grid cell.

The simulated total runoff for the last two years run was provided to the river routing model. We initialized the rivers with zero water, and spun the system up for four years with 1987 results, until the river discharges became cyclic. Another year was run, for 1988 conditions, continuing from the end of 1987. River discharges simulated for the last two years have been used to analyze the surface water balance at river-basin scale, and are discussed in following sections.

4. Results and analyses

4.1 Annual soil moisture and water balance for global and regional scales

Figure 1a shows the simulated 1987 and 1988 two-year annual mean soil moisture (mm) in the three soil layers. The annual-mean results clearly show that there was more soil moisture in tropical and temperate regions than in deserts and other relatively dry regions. The soil wetness, which is the fraction of the soil moisture saturation relative to the soil's water-holding capacity, is shown in Fig. 1b. The soil is more saturated in high latitudes, eastern North America, South America, East and Southeast Asia, and tropical Africa.

There were significant interannual changes of soil moisture between the two years of the simulations. Figure 1c shows the relative differences of the annual mean soil moisture (percent) between 1988 and 1987, divided by the soil moisture in 1987. In most of the midlatitudes of the Northern Hemisphere, the soil was much drier in 1988 than in 1987, showing about a 15 %–30 % decrease. In northern Australia, the soil was about 40 % to 50 % drier in 1988 relative to 1987. On the other hand, in some semi-desert regions, we see increased soil moisture in 1988. Interannual variations of soil moisture were also observed at local stations in Eurasia, and will be discussed in Section 4.3. The differences in soil moisture correlate well with differences in annual precipitation (not shown). One exception is northeast India, where a rainy 1988 did not result in higher soil moisture for 1988.

The temporal standard deviation of the monthly means for two years of the simulated soil moisture are shown in Fig. 1d, indicating seasonal variations of soil moisture. Generally, there were large seasonal variations in tropical and subtropical regions, ranging from 15 % to 50 % relative to the two-year mean value. In mid- and high latitudes, seasonal soil moisture variations were generally small, under 10 % relative to the annual mean, due to less potential evaporation in those regions.

Figure 2 shows the simulated river discharges for the basins, and comparisons with long-term river discharge observations. Observations for the basins were collected at gauge stations. Each gauge station measured one major catchment in its basin. These data were compiled by Oki (1998). For this study, because the forcing data, such as precipitation, temperature, and surface downward radiation fluxes, were specified from observations or from estimates based on the ECMWF model output, and so are presumed reliable, we expect the most realistic estimates of soil moisture to be obtained where the surface water balance is in a good agreement with the observations. The total areal coverage of the sixty-nine basins is about 6317.3 (10^{10} m^2), which is 48 % of the Earth's land area (vegetated and bare soil).

The simulated river discharges for most basins agree reasonably well with the observed river discharges, although the simulation produces underestimates for large river discharges, and overestimates for small river discharges. The averaged annual mean discharge values for the sixty-nine major rivers were 242 and 270 mm for the simulation and observations, respectively, *i.e.*, the simulated values are about 10 % less than observed. For three of the basins, the implied error in precipitation minus evaporation is greater than 1 mm day^{-1}.

Figure 3 shows ratios of the simulated discharges over precipitation forcing, compared with the ratios of the observed river discharges over climate precipitation from Legates and Wilmont (1990b). Although time periods for the long-term river dis-

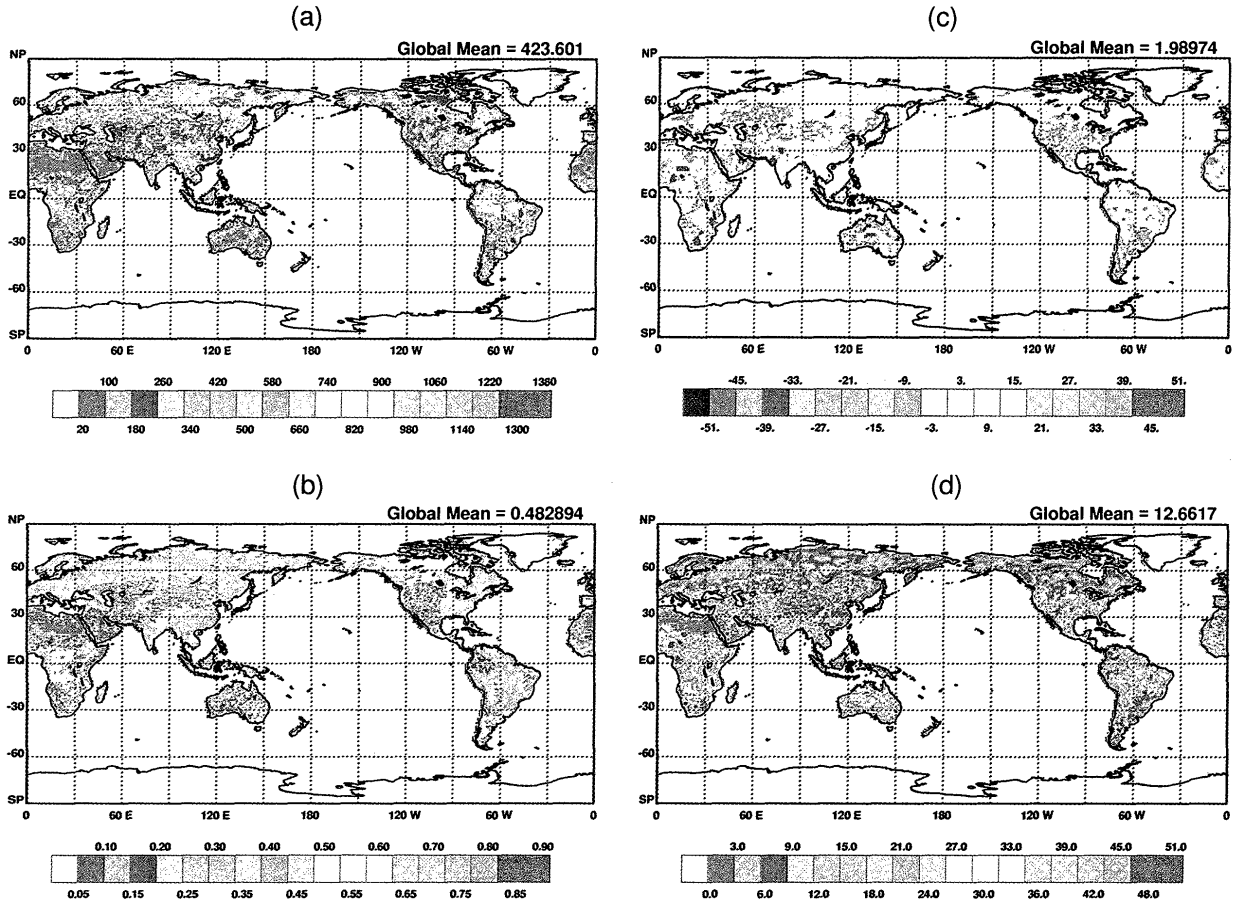

Fig. 1. (a) Distributions of the total simulated two-year annual mean soil moisture (mm) in the three soil layers combined; (b) Soil wetness as a fraction of the saturation soil moisture relative to the soil water holding capacity; (c) Differences of the annual soil moisture (percent)between 88 and 87, relative to 87; (d) The temporal standard deviation as a percentage of the mean for 87 and 88, indicating seasonal changes of soil moisture.

charge and precipitation observations were not exactly same, we use them as climatological statistics for this study. This alternative representation of the discharge allows its role to be compared to that of evaporation; the evaporation to precipitation ratio is one minus the discharge-to-precipitation ratio. In general, the model overestimated the discharge-precipitation ratio for small observed ratios, and underestimated it for large observed ratios. Too much discharge implies not enough evaporation and vice versa, assuming correct precipitation forcing.

Figure 4 compares the simulated basin-averaged annual surface evaporation with the ECMWF-simulated surface evaporation. This comparison will not tell what the "true" evaporation was, because of the dramatically different surface land-surface schemes used in the ECMWF data-assimilation system (Blondin, 1988; ECMWF, 1987) and in the model used in this study. However, comparing these two evaporation datasets may help explain the simulated surface water balance, because the same ECMWF data assimilation products are used as surface meteorological and radiation forcing. For most of the sixty-nine river basins, the annual surface evaporation was underestimated compared with the ECMWF results. This is partly due to the stronger surface control on transpiration imposed by stomata over vegetated land (Randall *et al.*, 1996; Sellers *et al.*, 1996; Zhang *et al.*, 1996), and also due to excessive surface evaporation produced by the ECMWF model, as discussed by Blondin (1988).

4.2 Seasonal cycle of soil moisture and water balance for selected river basins

Figure 5a shows the simulated soil moisture and water balance, and comparisons with observations, for the Amazon basin (619×10^{10} m^2). The simulation shows that the Amazon basin soil was wetter in the rainy season and drier in the dry season, following the annual precipitation cycle. The soil moisture difference between wet and dry seasons was more than 110 mm of soil water. The simulated surface evaporation agreed well with the ECMWF model

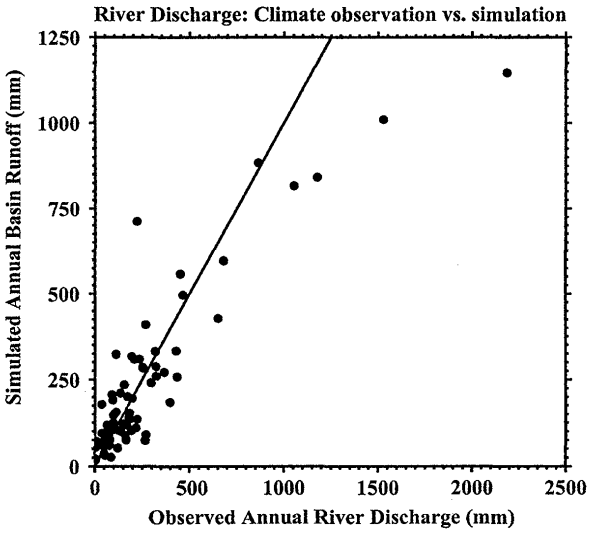

Fig. 2. Simulated river discharges for some major river basins, and their comparison with long-term river discharges observed at catchment gauge stations in the basins.

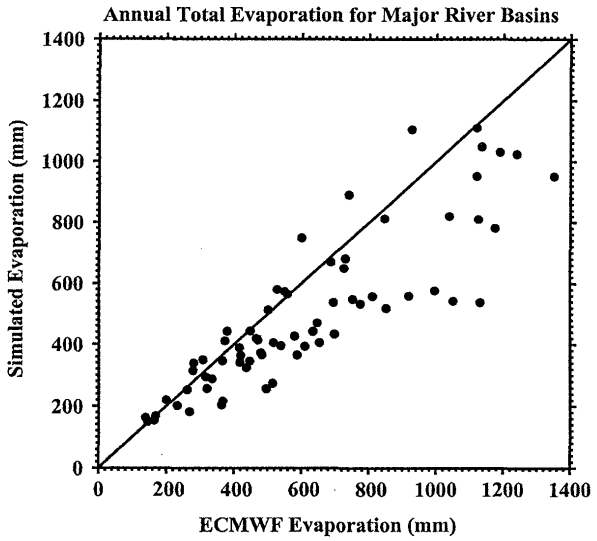

Fig. 4. A comparison of the simulated basin-averaged annual surface evaporation with the ECMWF-simulated surface evaporation.

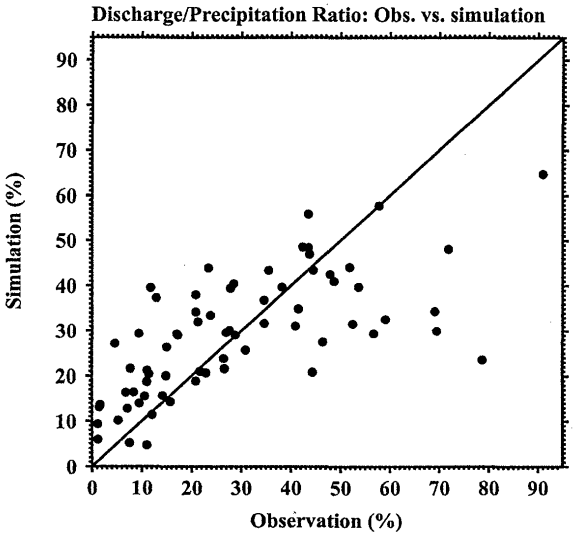

Fig. 3. A comparison of ratio of the simulated discharge over precipitation forcing with the ratio of the observed river discharge over climate precipitation from Legates and Wilmont (1990b).

output in the annual mean, but shows some differences in the seasonal cycle. The simulation produced less evaporation than the ECMWF model in the first eight months of the year, and more evaporation in later months.

Using river discharge data, we indirectly estimated water balance at the basin scale, when the other water balance components were not completely observed. To analyze the river discharge data, we used model-produced total runoff to force the river routing model, as discussed in Section 2. As shown in Fig. 5a, the simulated river discharge compares reasonably well with the observations at the Amazon river mouth. The time of peak discharge corresponds well with the observations. In the annual mean, the simulation produces less discharge than observed. Comparing monthly climatological precipitation (Legates and Willmott, 1990b) with the two-year precipitation used in our simulation, the two-year precipitation was less than climatology by about the amount that the discharge is underestimated. Thus, it is consistent with the river discharge comparison, and shows the seasonal cycles of soil moisture and water balance at the Amazon basin were reasonably simulated after accounting for the differences between the forcing and the climatology.

For the much smaller Chao Phraya river basin (16×10^{10} m^2) in Southeast Asia, Fig. 5b shows the simulated soil moisture and water balance and comparisons with observations. For the Chao Phraya basin, soil moisture increases and decreases closely following the annual precipitation cycle, with wetter soil in the rainy season and drier soil in the dry season. The soil moisture differences between wet and dry seasons are on the order of 200 mm. The simulated monthly surface evaporation agrees well with the ECMWF model output, although there is less evaporation than in the ECMWF model output for the dry season, and the simulated minima and maxima precede those of ECMWF model by about a month.

The simulated river discharge and the observations are also shown. The simulated river discharge

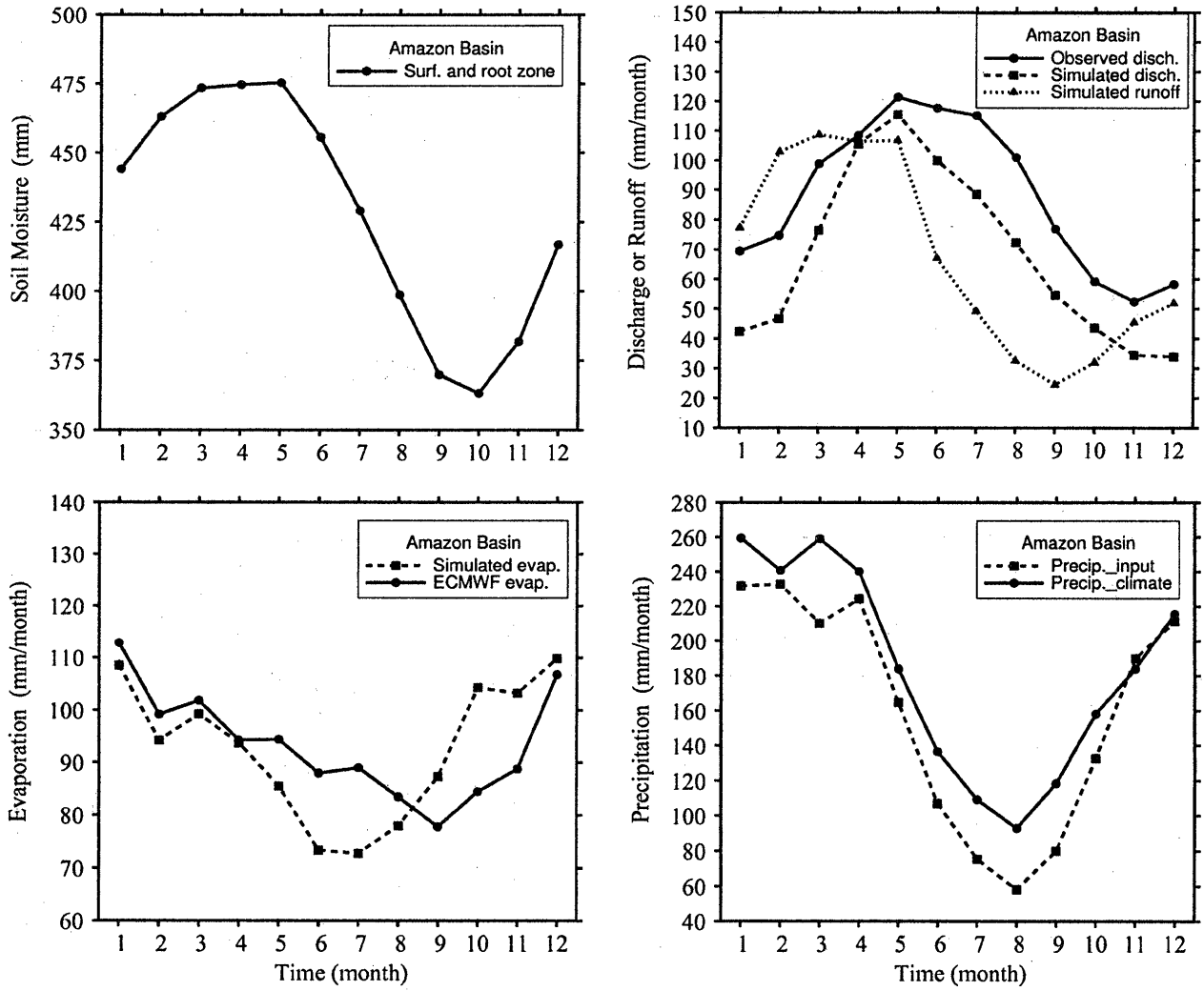

Fig. 5a. Comparisons of the simulated soil moisture and water balance with observations for the Amazon basin.

compares reasonably well with observations at the river mouth. The peak discharge matches well with the observations, but with stronger discharges than observed for September and October. The seasonal cycles of the simulated discharges are similar, with little phase difference, because of the relatively short river routes of the Chao Phraya river basin. Overall, the simulation agrees well with the observations, even though the observations and simulation cover different time periods. Comparing monthly climate precipitation (Legates and Willmott, 1990b) with the two-year precipitation forcing, the two-year forcing data also agrees well with climatology. Thus, the seasonal cycles of soil moisture and water balance for the smaller Chao Phraya basin also were simulated reasonably.

The Mississippi river has been chosen as a representative midlatitude river and its soil moisture and water balance have been compared with observations (Fig. 5c). Seasonal variations of soil moisture show a wetter soil in winter and spring and a drier soil in summer and early fall. The soil moisture is responding to both evaporation and snow accumulation/melting. The amplitude of the seasonal cycle of soil moisture is smaller than for the two tropical basins, with a range of about 70 mm. The simulated monthly surface evaporation is less than the ECMWF model output most of time, except in August, September, and October. This reflects the excessive surface evaporation and cooler surface air temperature predicted by ECMWF model (Blondin, 1988), with larger errors in mid- and high latitudes. When using the ECMWF-predicted surface air temperature to force the model in offline simulations, surface evaporation is underestimated, and snow accumulation and melting were delayed.

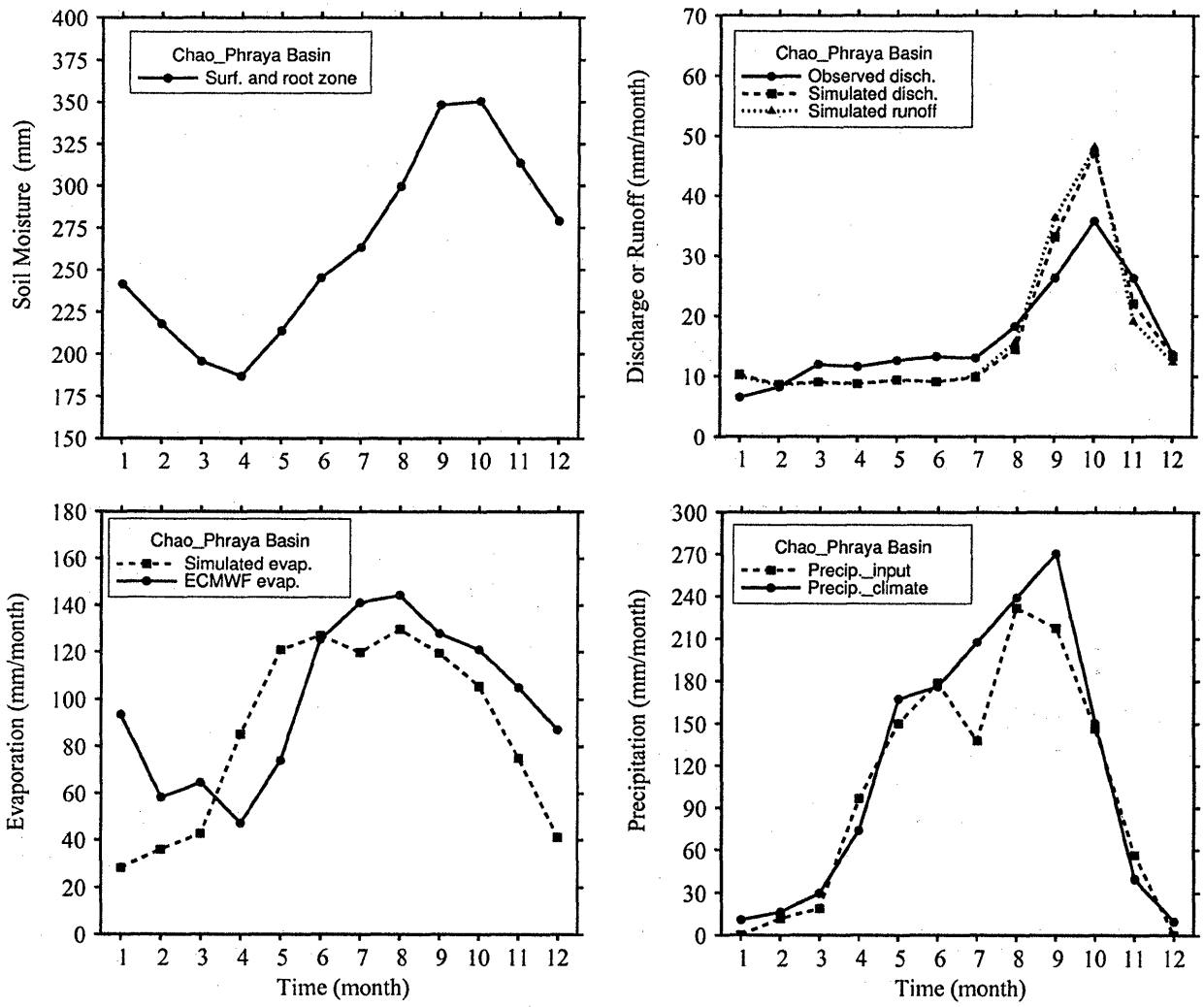

Fig. 5b. Same as Fig. 5a, but for the Chao Phraya river basin.

Comparing monthly climatological precipitation (Legates and Willmott, 1990b) with the two-year precipitation forcing, the two-year precipitation was less than the climatology. With less precipitation and less surface evaporation, the net effect on the surface water balance is reduced. In a comparison between the simulated river discharges and the observations, the simulated water balance for the Mississippi basin compared reasonably well with the observations. The peak discharge corresponded well with the observations, with stronger discharge in spring and less discharge in late summer. The weak discharge in spring was attributed to much less snow accumulation in winter and less snow melt in spring, compared with ten years of satellite observations (Fig. 6). Generally, the seasonal cycles of the soil moisture and water balance for the Mississippi river basin were reasonably well simulated, given the limitations of the forcing data.

Figure 5d shows the simulated soil moisture and water balance, and comparisons with observations, for the Mackenzie river basin. The Mackenzie river flows into the Arctic Ocean. The seasonal cycle of soil moisture shows a wet soil in spring and summer and a dry soil in winter. The soil moisture responds to both evaporation and snow accumulation/melting. The amplitude of the seasonal change of soil moisture becomes smaller still, compared to lower latitudes, with a range of about 50 mm. The simulated monthly surface evaporation was less than in the ECMWF model output for spring, and was more in late summer and early fall. This again reflects the excessive surface evaporation and cooler surface air temperature predicted by the ECMWF model (Blondin, 1988), with larger errors in mid- and high latitudes. When we used the ECMWF-predicted surface air temperature to force the model, surface evaporation is underestimated, and snow ac-

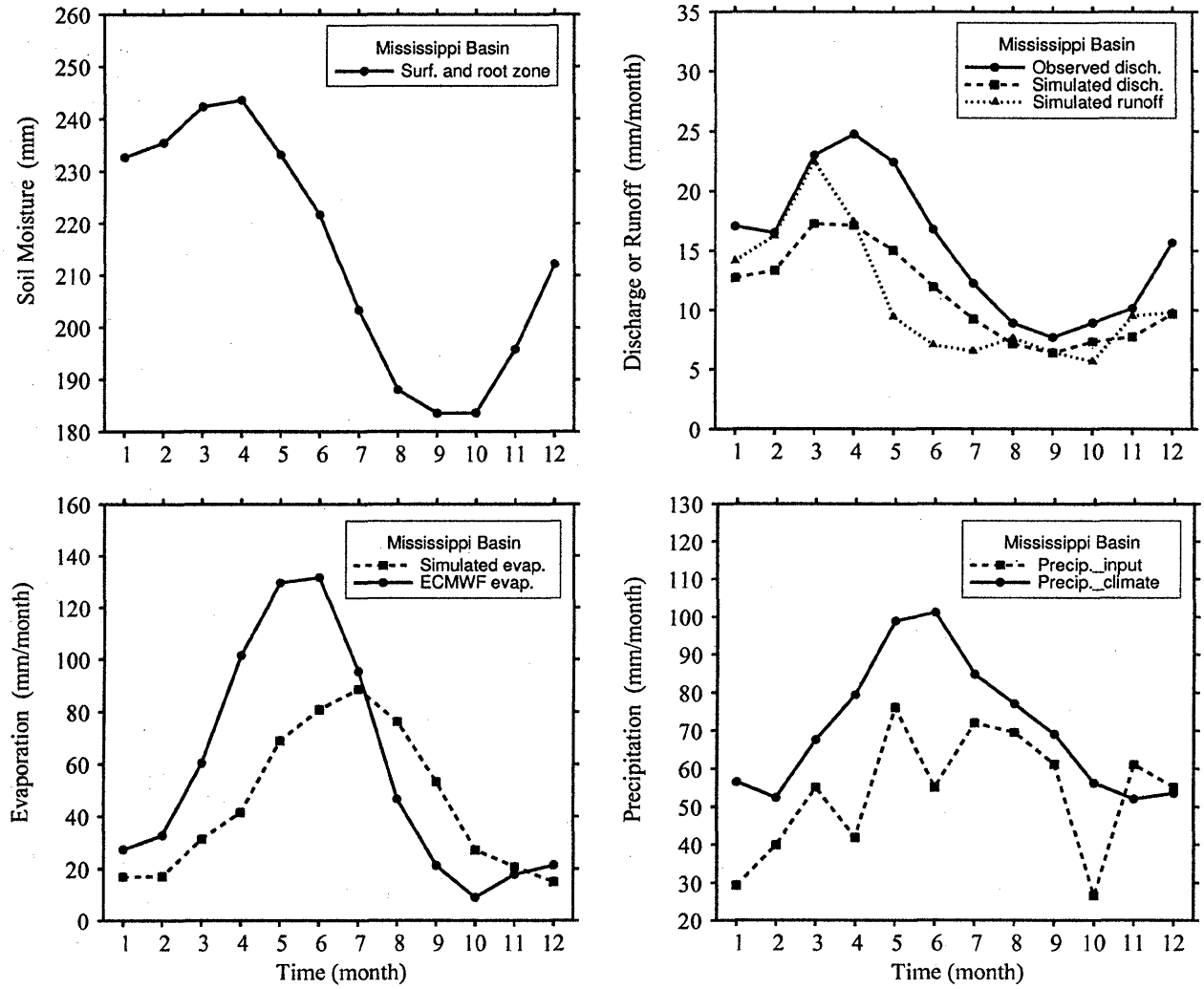

Fig. 5c. Same as Fig. 5a, but for Mississippi river basin.

cumulation and melting processes are delayed.

When comparing monthly climatological precipitation (Legates and Willmott, 1990b) with the two-year precipitation forcing, there was more precipitation in the two-year forcing than in climatology. With more precipitation forcing and less simulated evaporation in spring and summer, we expected the total runoff for the basin to be overestimated during that time. Looking at the simulated river discharges and the observations, the amplitude of water balance simulated for the Mackenzie river basin compares reasonably well with the observations, but with the peak discharge rate delayed by about one month. A late snow melt may contribute to the late river discharge, and in fact the onset of simulated snow melt in spring lags the ten-year satellite observations by about a month (Fig. 6). The 20 mm of snow melt observed but not simulated between March and April compares well in magnitude to the difference in observed and simulated discharge later in spring.

4.3 Seasonal cycle of soil moisture and water balance at local stations

For selected grid cells, the simulated soil moisture and water balance have been analyzed by comparing simulations with available observations at local stations.

Figure 7 shows the simulated soil moistures in top 0.5 and 1.0 m layers, and comparisons with corresponding observations at six locations located across Eurasia. The six locations are listed in Table 1. The soil conditions and vegetation types for these locations were discussed by Robock *et al.* (1995) and Vinnikov and Yeserkepova (1991). Also included in the table for comparison are the vegetation types and soil parameters used in the model.

To compare the simulations with observations,

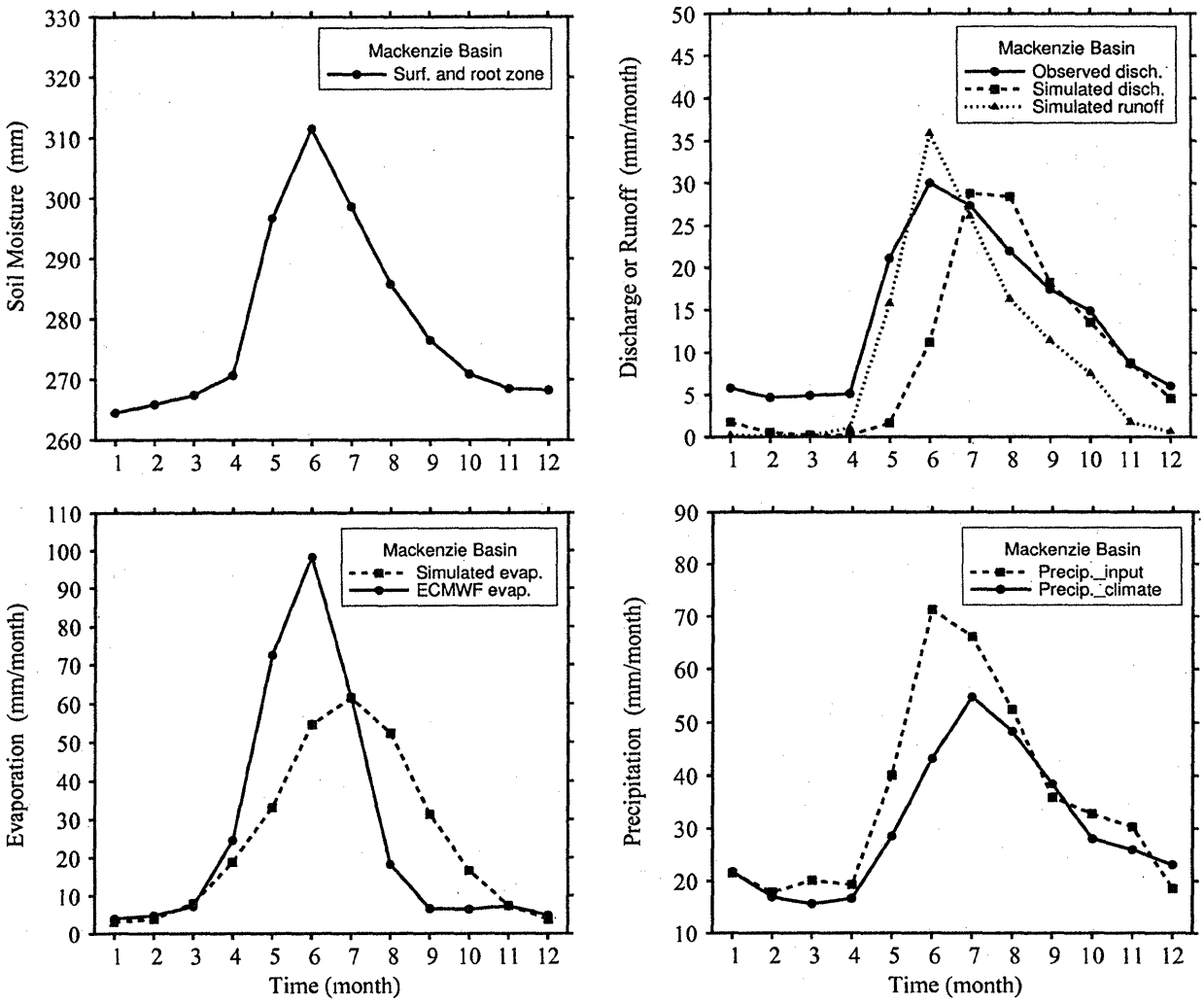

Fig. 5d. Same as Fig. 5a, but for Mackenzie river basin.

soil moistures simulated in the top 0.5 and 1.0 m soil layers were calculated from the surface and root-zone layers in the model by interpolation. First, the soil wetness for the simulated soil moisture was calculated for the top two soil layers. These two soil wetness values were then interpolated to obtain values characteristic of the top 0.5 and 1.0 m of the soil.

In Fig. 7, the simulated and observed soil moisture averaged over ten-day periods are shown for a seasonal cycle. The standard deviations of the interannual variability of the observed data were calculated, based on six years of observations from 1978 to 1983. There were large interannual variations of soil moisture for the top 0.5 and 1.0 m soil layers, for all six locations. The general characteristics of the observations are that soil moisture reaches a peak value in spring due to snow melt, then decreases during the summer months, and finally recharges in the fall.

The simulated soil moisture was for the two-year averaged values for 1987 and 1988. The model produced soil moistures with fair-to-good agreement in the phase of the seasonal cycle at the six locations, except for Tulun, where little seasonal cycle was simulated. However, the two-year simulation shows a much smaller amplitude of the seasonal cycle than observed, particularly at Khabarovsk and Kostroma. For Orgurtsovo, Uralsk, and Yershov, the simulation shows better agreement with the observations for both soil layers, with a stronger spring soil moisture maximum, following a deep withdrawal of soil moisture in summer, and recharging of soil moisture in fall, although the simulated soil moisture decrease is about one month later than observed, and also soil moisture recharge is much weaker than observed in fall. As a result, the simulated soil moisture was less than observed in winter.

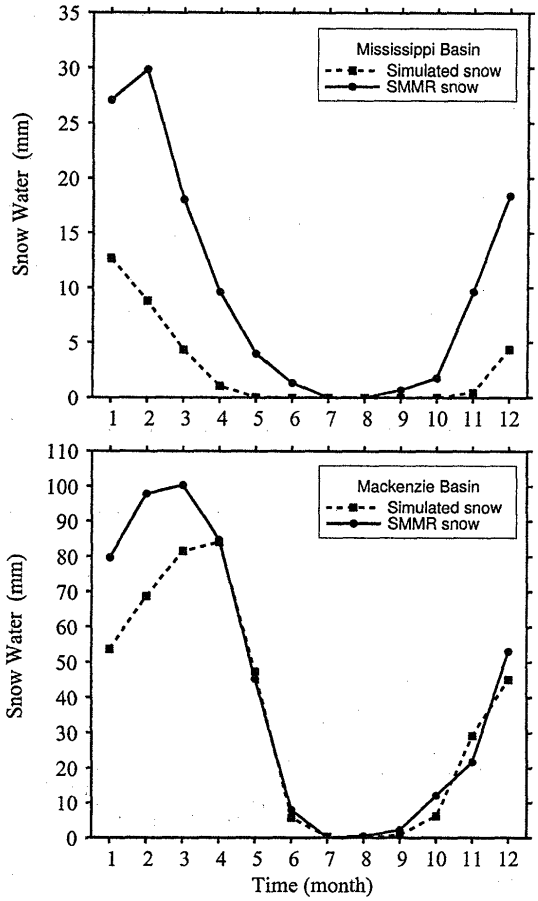

Fig. 6. Comparisons of the simulated snow accumulation/melting with satellite observations for the Mississippi and Mackenzie river basins.

The annual-mean soil moistures for the simulations and observations at the six locations are listed in Table 2. At four of the sites (Khabarovsk, Kostroma, Uralsk, and Yershov) the agreement is good when the difference in holding capacity (Table 1) is accounted for, and the annual-mean differences between the simulation and observations are within the multi-year ranges observed at the stations (Fig. 7). However, the simulations at Ogurtsovo and Tulun were too moist in absolute terms, and the smaller simulated holding capacity made the relative error worse.

This type of comparison is very challenging for the model, because we are comparing very different years of the simulation and the observation, and the soil and vegetation parameters assigned to a grid cell can differ from those at specific sites located within the cell.

Figure 8 presents the simulated snow water equivalent, and a comparison with observations for the corresponding stations. Comparing two observational data sets obtained by on-site observations and satellite remote sensing with the Scanning Multichannel Microwave Radiometer (SMMR, Chang *et al.*, 1990, 1992), we find that the remotely sensed observations overestimated snow water for Khabarovsk and Tulun. The satellite data cover the period from 1978 to 1987, and were averaged to obtain a ten-year-mean seasonal cycle. The simulated snow water equivalent compared reasonably well with the station and the remotely sensed observations at most of the locations. The timing of the simulated snow accumulation agrees well with the observations. On the other hand, the initiation of the simulated net snow melt shows a one-month lag relative to the observations, for all but the Ohurtsovo station. This may have contributed to the late soil moisture withdrawal in spring and early summer, as shown in Fig. 7.

Figure 9a compares the precipitation used to force the simulation with the precipitation observed at the six stations. The precipitation forcing agrees well with the station observations. As discussed earlier, the precipitation forcing is based on monthly observations for 1987 and 1988, interpolated into 6-hourly value by using the NCEP-forecast precipitation for the same period. It is quite likely that the intensity of precipitation events is underestimated due to the temporal interpolation and to the use of a grid-cell average value for the forcing.

The temperature forcing for this study is compared with local observations in Fig. 9b. For most of the six locations, the specified air temperature was cooler than observed in winter and spring. This was due to the excessive surface evaporation in the ECMWF forecasting system, as reported by Blondin (1988). As a result, the simulated snow melt at the associated grid cells was about one month later than observed as described above. This may have contributed to a later and smaller simulated soil moisture withdrawal due to under-simulated evaporation. That would reduce the amplitude of the seasonal cycle.

5. Summary and conclusions

We have simulated the seasonal and annual cycles of soil moisture and surface water balance at global and regional scales using a land-surface process model (SiB2) forced by observed and assimilated data. The simulated runoff data were provided, as input to a global river-routing model, to compute river discharge rates. The simulated soil moisture and water balance were compared with available observations at various spatial scales. Given the characteristics of each dataset, it is encouraging that the simulated seasonally varying soil moisture and water balance agrees reasonably well with observations. Due to excessively cool temperatures in the forcing data, the simulated surface evaporation was smaller and the seasonal cycle of evaporation was about one month late, compared with the ECMWF model out-

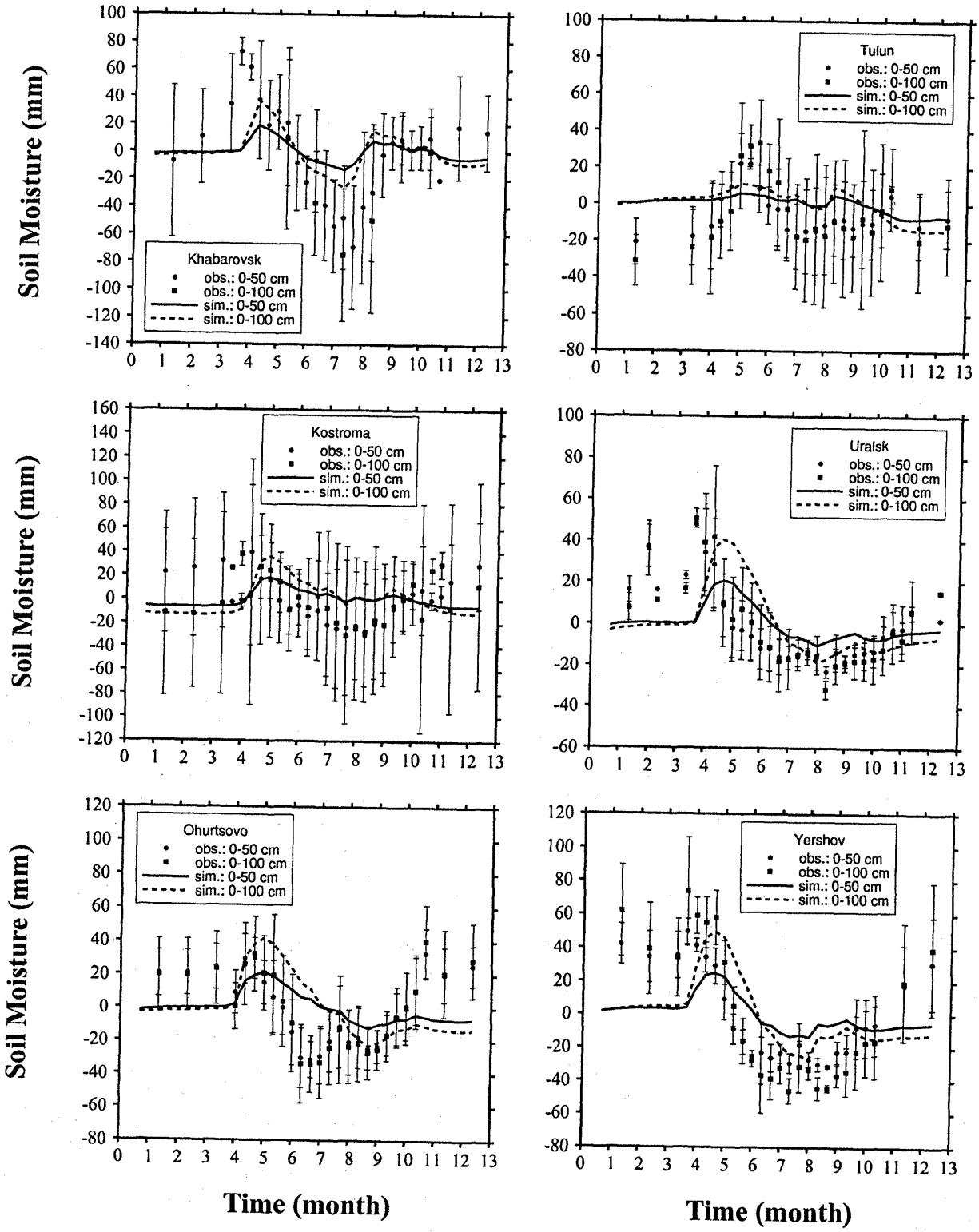

Fig. 7. A comparison of the seasonal cycle of the simulated soil moisture with observations for six stations. The error bars represent plus or minus one standard deviation of the interannual variation, using six years of data for each station, from 1978 to 1983.

put. There were some fundamental differences between the version of the land-surface model used in the ECMWF system and SiB2; the latter imposes stronger stomatal controls on the surface transpiration. However, the erroneously cool temperatures tend to have a strong effect on the simulated soil moisture and surface water balance, in agreement with Milly (1992).

Table 1. Observation station names, locations and water holding capacities (mm), and SiB2 model vegetation used.

Location	Lat., Lon.	Observed soil water holding capacity: top 500/1000 (mm)	SiB2 water holding capacity: top 500/1000 (mm)	Vegetation Type Observed/SiB2
Khabarovsk	48.5°N, 135.2°E	262/ 483	219/ 439	grass/needleleaf and deciduous trees
Kostroma	57.8°N, 41.0°E	N/A	219/ 439	grass/needleleaf trees
Ogurtsovo	54.9°N, 83.0°E	286/ 557	232/ 465	grass/deciduous trees over wheat
Tulun	54.6°N, 100.6°E	302/ 548	219/ 439	grass/needleleaf trees
Uralsk	51.3°N, 51.4°E	271/ 483	219/ 439	grass/deciduous trees over wheat
Yershov	51.4°N, 48.3°E	256/ 464	219/ 439	grass/deciduous trees over wheat

Table 2. Annual mean soil moisture in top 500 and 1000 mm layers for observations, simulations, and their differences, at six selected station and associated grids.

Location	Obs. in top 0.5 m layer	Sim. in top 0.5 m layer	Obs. minus sim.	Obs. in top 1.0 m layer	Sim. in top 1.0 m layer	Obs. minus sim.
Khabarovsk	201.5	162.4	39.1	401.5	325.9	75.6
Kostroma	193.5	164.1	29.4	343.7	328.9	14.8
Ogurtsovo	112.8	164.8	−55.6	227.4	338.1	−110.7
Tulun	128.5	154.4	−25.9	261.5	309.5	−48.0
Uralsk	80.9	76.6	4.3	182.7	154.0	28.7
Yershov	86.9	90.0	− 3.1	192.4	180.5	11.9

The observed global distributions of the annual mean soil moisture and wetness were reasonably well simulated. The seasonal variations of soil moisture are large in tropical and sub-tropical regions, but small in mid- and high latitudes. There are large inter-annual variations of soil moisture in both the simulation and the observations. The simulated annual discharge amounts for major river basins agree reasonably well with the observations, although the simulation tends to underestimate for large discharge and overestimate for small discharge.

The seasonal cycles of soil moisture and water balance for river basins and individual grid cells were reasonably well simulated for locations in tropics, midlatitudes, and high latitudes. In tropics, the seasonal cycles of soil moisture and surface water balance were dominated by the precipitation cycle. The soil was wet or dry following rainy and dry seasons, respectively. Soil moisture and water balance for both a large river basin (the Amazon) and a small river basin (the Chao Phraya) were also reasonably simulated. In mid- and high latitudes, the cycles of soil moisture and water balance were affected by temperature and precipitation, where snow accumulation/melting became important. The soil was dry in summer and wet in winter and spring. The range of seasonal soil moisture changes became smaller at higher latitudes.

For selected grid cells, the simulated seasonal cycles of soil moisture were compared with station observations. Although there were differences in meteorological forcing and in some specific surface boundary parameters, the annual-mean simulated soil moisture agreed favorably with multi-year observations at four of six locations. The phase of the seasonal cycle agreed well for almost all locations. However, for almost all the selected grid cells, the seasonal variations were smaller, snow melting and soil drying were delayed by about one month, and the soil was relatively wetter in summer, compared with the observations.

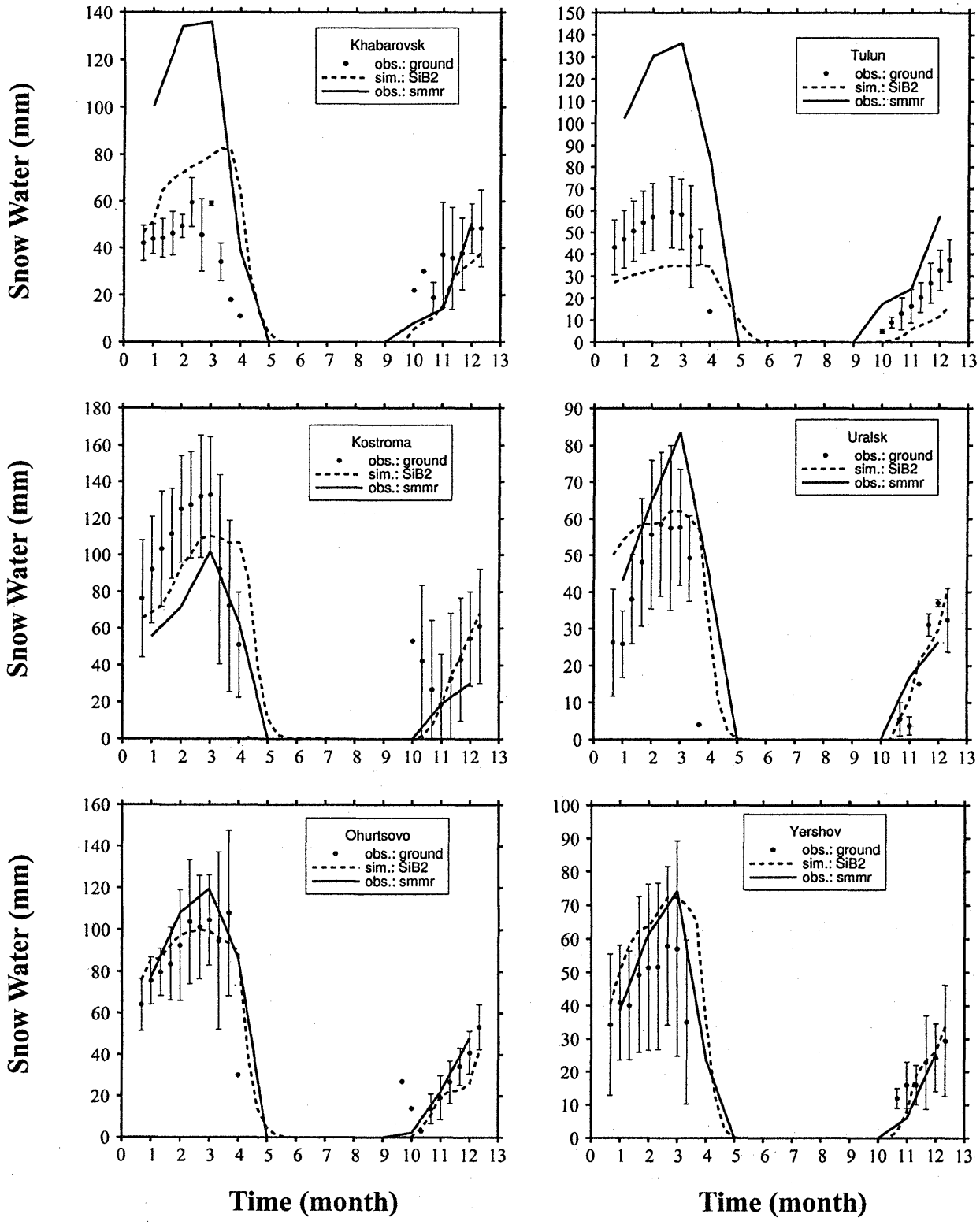

Fig. 8. Comparisons of the simulated snow water equivalent with station observations obtained at stations and with satellite observations.

Acknowledgments

We thank Alan Robock and Adam Schlosser for providing the station soil moisture data sets. We are grateful to Jasmin John for providing the code for the river-routing model, and to Taikan Oki for providing the TRIP data. This study benefited greatly from our discussions with Taikan Oki, Gary Russell, and Jasmin John. The comments of the reviewers

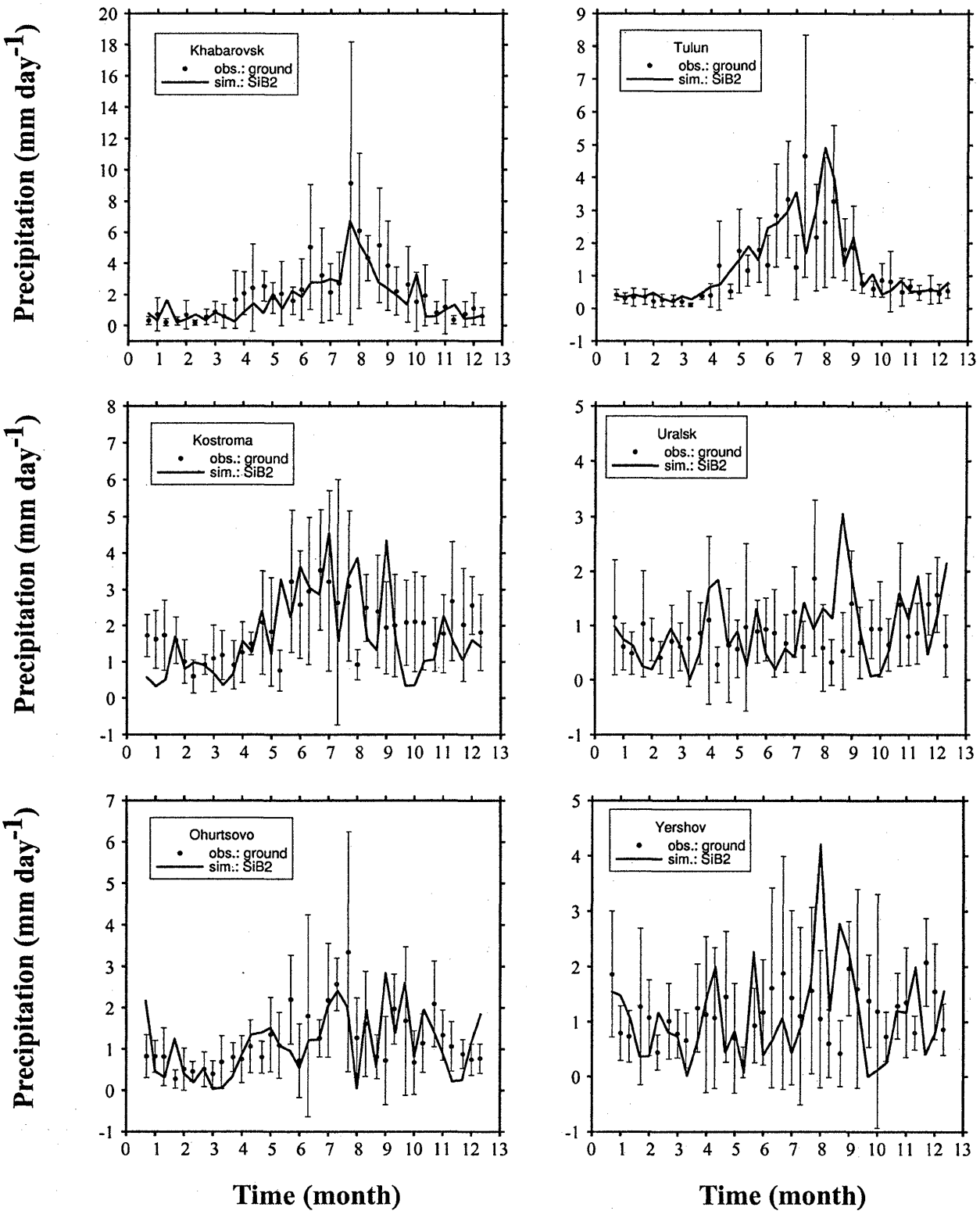

Fig. 9a. Comparisons of the grid-averaged precipitation forcing with the observed precipitation at the six stations.

were invaluable in improving the focus and clarity of this paper. This work has been supported by NASA's Earth Observing System (EOS) program, through the NASA Contract number NAS5-31730.

References

Betts, A.K., J.H. Ball, A.C. Beljaars, M.J. Miller and P. Viterbo, 1994, Coupling between land surface, boundary layer parameterizations and rainfall on lo-

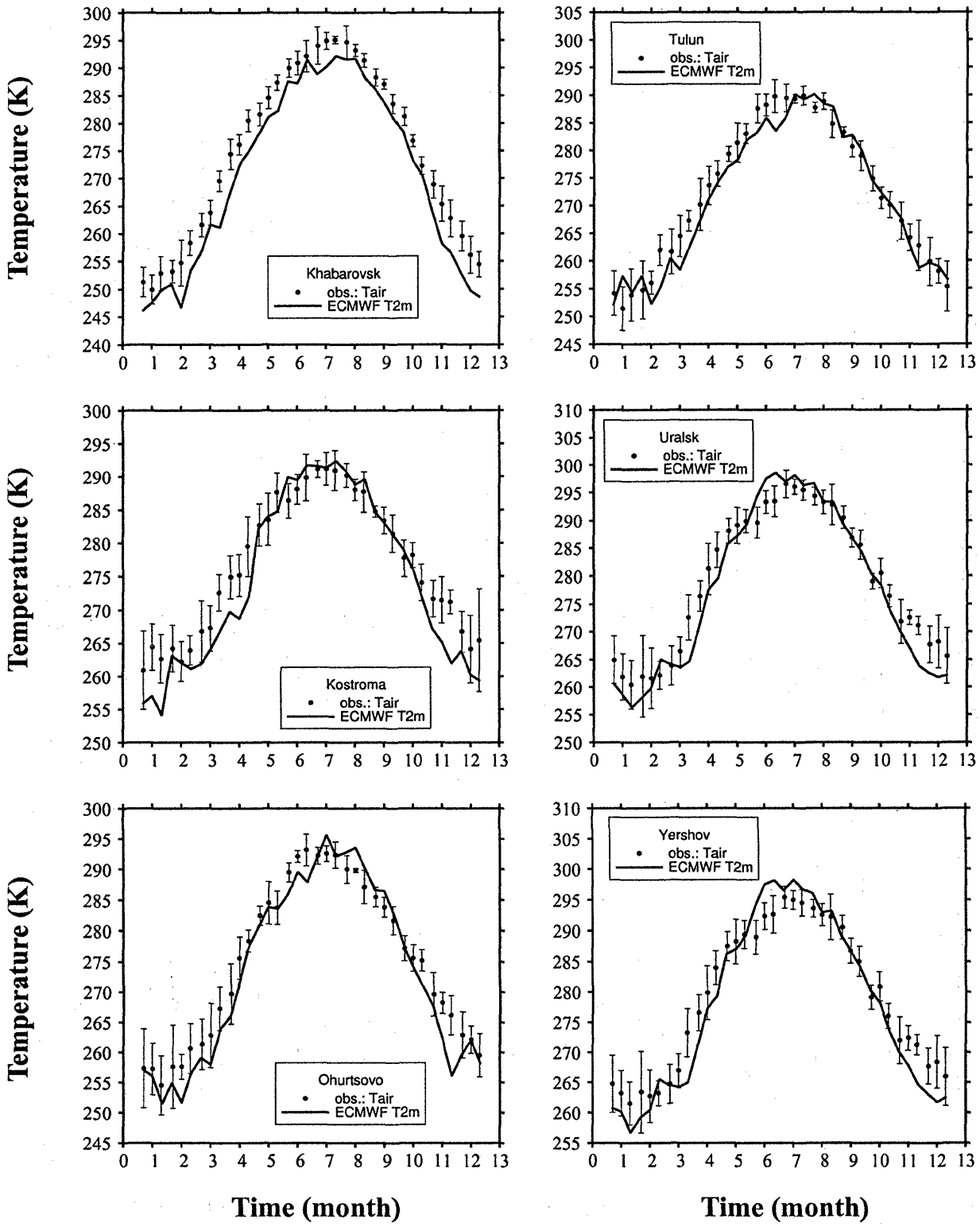

Fig. 9b. A comparison of the grid-averaged 2 m air temperature forcing with local station observations.

cal and regional scales: Lesson from the wet summer of 1993. *Fifth Conference on Global Change Studies, Amer. Meteor. Soc.*, 74th Annual Meeting. Nashville, Tenn., Jan 23–28.

Blondin, C., 1988, Research on land surface parameterization schemes at ECMWF, in *ECMWF Workshop Proceedings: Parameterization of Fluxes Over Land Surface*, 24–25 Oct.

Budyko, M.I., 1956, Heat balance at the earth's surface, Gidrometeoizdat, Leningrad, 225pp.

Chang, A.T.C., J.L. Foster, D.K. Hall, H.W. Powell and Y.L. Chien, 1992, Nimbus-7 SMMR Derived global snow cover and snow depth dataset documentation, product description, and user's guide. *The Pilot Land Data System.* Goddard Space Flight Center, Greenbelt, Maryland.

Chang, A.T.C., J.L. Foster, D.K. Hall, 1987, Nimbus-7 SMMR derived global snow cover parameters, *Ann. Glaciol.*, **9**, 39–44.

Chang, A.T.C., J.L. Foster, D.K. Hall, 1990, Satellite estimates of Northern hemisphere snow volume, *Remote Sensing Letters, International Journal of Remote Sensing*, **11**, 167–172.

Collatz, G.J., J.A. Berry, G.D. Farquhar and J. Pierce, 1990, The relationship between the rubisco reaction mechanism and models of leaf photosynthesis, *Plant Cell Environ.*, **13**, 219–225.

Collatz, G.J., J.T. Ball, C. Grivet and J.A. Berry, 1991, Physiological and environmental regulation of stomata conductance, photosynthesis and transpiration: a model that includes a laminar boundary layer, *Agric. Forest Meteo.*, **54**, 107–136.

Collatz, G.J., M. Ribas-Carbo, J.A. Berry, 1992, Coupled photosynthesis-stomatal conductance model for leaves of C4 plants, *Aust. J. Plant Physiol.*, **19**, 519–538.

Delworth, T.L. and S. Manabe, 1988, The influence of potential evaporation on the variabilities of simulated soil wetness and climate. *J. Climate*, **1**, 523–547.

Delworth, T.L. and S. Manabe, 1989, The influence of soil wetness on near surface atmospheric variability. *J. Climate*, **2**, 1447–1462.

Denning, A. S., G. J. Collatz, C. Zhang, A.A. Randall, J.A. Berry, P.J. Sellers, G.D. Colello and D.A. Dazlich, 1996, Simulations of terrestrial carbon metabolism and atmospheric CO_2 in a general circulation model, Part 1: Surface carbon fluxes. *Tellus*, **48B**, 521–542.

Dickinson, R.E., 1984, Modeling evapotranspiration for the three-dimensional global climate models, in *Climate Processes and Climate Sensitivity*, J. Maurice Ewing Ed., **5**, Amer. Geophys. Union, 58–72.

Dickinson, R.E., 1995, Walter Orr Roberts Lecture: Land surface processes and climate modeling. *Bull. Amer. Meteor. Soc.*, **76**, 1445–1448.

Dirmeyer, P.A., 1994, Vegetation stress as a feedback mechanism in midlatitude drought. *J. Climate*, **7**, 1463–1483.

ECMWF, 1987, ECMWF data assimilation — Scientific documentation, *Research manual version 2.* Ed. by Lonnberg and Shaw Eds.

Fennessy, M.J., J.L. Kinter III, L. Marx, E.K. Schneider, P.J. Sellers and J. Shukla, 1994, GCM Simulations of life cycles of the 1988 U.S. drought and heat wave. *COLA Report 6*, Center fir Ocean-Land-Atmosphere Studies, Calverton, MD. pp. 68.

International GEWEX Project Office, 1995, Global Soil Wetness Project. Version 1.0. *International GEWEX project Office*, December 1.

Kunkel, K.E., S.A. Changnon and J.R. Angel, 1995, Climate aspects of the 1993 upper Mississippi River basin flood. *Bull. Amer. Meteor. Soc.*, **75**, 811–822.

Legates, D.R. and C.J. Willmott, 1990a, Mean seasonal and spatial variability in global surface air temperature, *Theor. Appl. Climatol.*, **41**, 11–21.

Legates, D.R. and C.J. Willmott, 1990b, Mean seasonal and spatial variability in gauge-corrected global precipitation, *Int. J. Climatol.*, **10**, 111–127.

Manabe, S., 1969, The atmospheric circulation and hydrology of the Earth's surface. *Mon. Wea. Rev.*, **97**, 739–774.

Miller, J.R., G.L. Russell, G. Caliri, 1994, Continental-scale river flow in climate models. *J. Climate*, **7**, 914–928.

Milly, P.C.D., 1992, Potential evaporation and soil moisture in general circulation models. *J. Climate*, **5**, 209–226.

Mintz, Y. and Y. Serafini, 1981, Global fields of soil moisture and surface evapotranspiration. *NASA Goddard Flight Center Tech. Memo. 83907*, Research Review-1980/81, 178–180.

Mintz, Y. and Y.V. Serafini, 1992, A global monthly climatology soil moisture and water balance. *Clim. Dyn.*, **8**, 13–27.

Mintz, Y. and G.K. Walker, 1993, Global fields of soil moisture and land surface evapotranspiration derived from observed precipitation and surface air temperature. *J. Appl. Meteor.*, **32**, 1305–1334.

Oglesby, R.J., 1991: Springtime soil moisture, natural climate variability, and North America drought as simulated by the NCAR Community Model 1. *J. Climate*, **4**, 890–897.

Oki, T. and Y.C. Sud, 1998, Design of the global river channel network for Total Runoff Integrating Pathway (TRIP), *Earth Interactions*, **2**. [Available online at http://EarthInteractions.org.]

Oki, T., 1998, The global water cycle, in "*Global Energy and Water Cycles*," K. Browning and R. Gurney Eds., Cambridge University Press, 10–27.

Randall, R.A., P.J. Sellers, J.A. Berry, D.A. Dazlich, C. Zhang, J.A. Collatz, A.S. Denning, S.O. Los, C.B. Field, I. Fung, C.O. Justice, C.J. Tucker and L. Bounoua, 1996, A revised land-surface parameterization (SiB2) for GCMs. Part 3: The Greening of the Colorado State University general circulation model, *J. Climate*, **9**, 738–763.

Rind, D., 1982, The influence of gound moisture conditions in North America on summer climate as modeled in GISS GCM. *Mon. Wea. Rev.*, **110**, 1487–1494.

Robock, A., K.Y. Vinnikov, C.A. Schlosser, N.A. Speranskaya and Y. Xue, 1995, Use of midlatitude soil moisture and meteorological observations to validate soil moisture simulations with biosphere and bucket models. *J. Climate*, **8**, 15–35.

Rowntree, P.R. and J.R. Bolton, 1983, Simulation of atmospheric response to soil moisture anomalies over Europe. *Quart J. Roy. Meteor. Soc.*, **109**, 501–526.

Sato, N., P.J. Sellers, D.A. Randall, E.K. Schneider, J. Shukla, J.L. Kinter III, Y-T, Hou and Albertazzi, 1989, Effects of implementing the simple biosphere model in a general circulation model, *J. Atmos. Sci.*, **46**, 2757–2782.

Sellers, P.J., D.A. Randall, C.J. Collatz, J.A. Berry, C.B. Field, D.A. Dazlich, C. Zhang, G. Collelo and L.

Bounoua, 1996 a, A revised land-surface parameterization (SiB2) for atmospheric GCMs. Part 1: Model formulation, *J. Climate*, **9**, 676–705.

Sellers, P.J., S.O. Los, C.J. Tucker, C.O. Justice, D.A. Dazlich, G.J. Collatz and D.A. Randall, 1996b, A revised land-surface parameterization (SiB2) for atmospheric GCMs. Part 2: the generation of global fields for terrestrial biophysical parameters from the NDVI, *J. Climate*, **9**, 706–737.

Seller, P.J., B.W. Meeson, J. Closs, J. Collatz, F. Corprew, D. Dazlich, F.G. Hall, Y. Kerr, R. Koster, S. Los, K. Mitchell, J. McManus, D. Myers, K.-J. Sun and P. Try, 1996c, The ISLSCP initiative I data sets: surface boundary conditions and atmospheric forcings for land-atmosphere study. *Bull. Amer. Meteoro. Soc.*, **77**, 1987–2005.

Shukla, J. and Y. Mintz, 1982, The influence of land-surface evapotranspiration on Earth's climate. *Science*, **215**, 1498–1501.

Vinnikov, K.Y. and I. B. Yeserkepova, 1991, Soil moisture: Empirical data and model results. *J. Climate*, **4**, 66–79.

Wood, E.F., D.P. Lettenmaier and V.G. Zartarian, 1992, A land surface hydrology parameterization with subgrid variability for general circulation models. *J. Geophys. Res.*, **97**, 2717–2728.

Zhang, C., D.A. Dazlich, D.A. Randall, P.J. Sellers and S.A. Denning, 1996, Calculation of the global land surface energy, water, and CO_2 fluxes with an off-line version of SiB2. *J. Geophys. Res.*, **101**, 19061–19075.

単純植生モデル2 (SiB2) による土壌水分と地表面水収支のシミュレーション

Changan Zhang・Donald A. Dazlich・David A. Randall
（コロラド州大学大気科学科）

観測ならびに同化データを地表面モデル (SiB2) に外力として与えることにより、グローバルおよび地域スケールでの土壌水分と水収支が算定された。各格子内で計算された流量は河川流出量を計算するためにグローバルな流下モデルの入力として与えられた。算定された土壌水分と水収支の年平均値と季節変化とが、グローバルスケールならびに格子点スケールで利用可能な観測値と比較された。シミュレーションにもローカルな観測にも土壌水分の大きな年々変動があった。主要な河川流域に対する年流出量算定値は観測値と概ね良く一致したものの、多い観測流出量に対してはやや過小推定もあり、少ない観測流出量に対してはいくらかの過大推定もあった。いくつかの河川流域では年平均値の過小評価があったものの、熱帯、中緯度、そして高緯度に特有の河川について河川流量の季節変化は良く再現されていた。熱帯では、土壌水分と地表面水収支の季節変化は降水量の季節変化に支配されている。中高緯度では土壌水分と水収支は気温と降水量の両者の季節変化と、積雪融雪変化の影響を受けている。緯度が上がるに連れて土壌水分の年変化幅は小さくなる。いくつかの格子点について推定した土壌水分の季節変化を観測点の数を変えながら比較した。観測点での観測外力と地表面パラメータにはモデルで利用したものと若干の違いがあるものの、算定された土壌水分はほとんどの観測地点で多年観測値と良く一致している。しかしながら、ほとんどの地点で、季節変化幅は観測値よりも小さく、融雪と土壌乾燥は一ヶ月程度遅く、土壌は夏季に比較的湿潤である。これらの誤差の一部は、外力としてモデルから与えられた気温が非現実的に低く、蒸発を抑制し特に中高緯度で季節進行を遅らせているためであると考えられる。